



# International Journal of Pharmacology

ISSN 1811-7775

**science**  
alert

**ansinet**  
Asian Network for Scientific Information



## Research Article

# Dysregulation of Inflammatory Cytokines by Endotoxin Induces Tissue iNOS Expression and Pulmonary Injury in Rats

<sup>1</sup>Fahaid Al-Hashem and <sup>2</sup>Amal F. Dawood

<sup>1</sup>Department of Physiology, College of Medicine, King Khalid University, Abha 61421, Saudi Arabia

<sup>2</sup>Department of Basic Medical Sciences, College of Medicine, Princess Nourah bint Abdulrahman University, P.O. Box 84428, Riyadh 11671, Saudi Arabia

## Abstract

**Background and Objective:** Pulmonary diseases are among the leading causes of mortality and disability worldwide and lower respiratory infections ranked as the fourth leading cause of death. This study aimed to the effects of three different doses of endotoxin on lung pathogenicity and selected the dose that induced the highest inflammatory response to investigate inflammation/nitrosative stress axis mediated lung injury. **Materials and Methods:** The model groups of rats were subjected to a single injection via Intra-Tracheal (IT) instillation of 5, 10 and 15 mg kg<sup>-1</sup> of endotoxin (En) and the control group received a saline injection. All rats were culled 3 days post endotoxin injection. **Results:** A severe acute lung injury was detected in all three experimental groups as revealed by a sharp increase in blood and/or lung tissue Granulocyte Monocyte-Colony Stimulating Factor (GM-CSF) levels, interleukin-6 (IL-6) and interleukin-17A (IL-17A). The order of potencies of the endotoxin's effects was: En15>En10>En5. En15 also (i) Demonstrated coagulopathy, including increased blood levels of prothrombin time (PT), plasminogen activator inhibitor (PAI-1), activated Partial Thromboplastin Time (APTT) and D-dimer, (ii) Caused >15 fold increase in lung tissue levels of nitrosative stress biomarker, Inducible Nitric Oxide Synthase (iNOS) and (iii) Induced lung tissue damage like a collapse of alveoli and interalveolar septal thickening. **Conclusion:** These findings demonstrated that endotoxin at 15 mg kg<sup>-1</sup> b.wt., induces after 3 days in rats a profound lung injury associated with the augmentation of the inflammation/iNOS axis, as well as coagulopathy biomarkers. Using this model may be useful for testing agents to treat severe acute lung damage.

**Key words:** Inflammation, nitrosative stress, endotoxin, pulmonary injury, alveolar collapse, thrombosis, coagulation

**Citation:** Al-Hashem, F. and A.F. Dawood, 2022. Dysregulation of inflammatory cytokines by endotoxin induces tissue iNOS expression and pulmonary injury in rats. *Int. J. Pharmacol.*, 18: 1412-1419.

**Corresponding Author:** Fahaid Al-Hashem, Department of Physiology, College of Medicine, King Khalid University, Abha 61421, Saudi Arabia  
Tel: 966-500142929

**Copyright:** © 2022 Fahaid Al-Hashem and Amal F. Dawood. This is an open access article distributed under the terms of the creative commons attribution License, which permits unrestricted use, distribution and reproduction in any medium, provided the original author and source are credited.

**Competing Interest:** The authors have declared that no competing interest exists.

**Data Availability:** All relevant data are within the paper and its supporting information files.

## INTRODUCTION

Acute Respiratory Distress Syndrome (ARDS) describes the severe type of acute lung injury mostly caused by blood infection<sup>1</sup>. It is a life-threatening syndrome characterized by inflammation, alveolar collapse and alveolar pulmonary oedema, as well as coagulation and abnormal chest x-ray that showed bilateral opacities 3 days following the insult<sup>2-4</sup>. Endotoxin (also known as lipopolysaccharide) is part of the Gram-negative bacteria cell wall structure that induces a severe immune response in humans and the role of endotoxin in ARDS pathology is well documented<sup>5</sup>. During ARDS, endotoxin activates the receptor, toll-like receptor-4, which recruits the infiltration of immune cells to the lung leading to the release of pro-inflammatory cytokines and hence induction of severe lung damage<sup>6</sup>.

Excessive production of free radicals like reactive oxygen species (ROS) as well as reactive nitrogen species (RNS) intricately in the pathophysiology of oxidative and nitrosative stress, respectively, which lead to tissue injury<sup>7</sup>. Induction of RNS via iNOS activation in acute lung injury is reported. For example, (i) Exposure of Wistar rats to nitrogen mustard caused damage to the respiratory system presented by infiltration of inflammatory cells, alveolar damage and fibrosis associated with the augmentation of lung tissue iNOS expression, which was protected by the iNOS inhibitor, aminoguanidine<sup>8</sup>, (ii) iNOS expression is increased in lungs of asthmatic patients<sup>9</sup> and (iii) iNOS expression is increased in rat alveolar macrophage following endotoxin administration and in human macrophage following chronic inflammation<sup>10</sup>. Therefore, this study anticipated the induction of the inflammation/iNOS axis mediated lung injury by endotoxin.

## MATERIALS AND METHODS

**Study area:** This study was carried out at the Research Centre, College of Medicine, King Khalid University, Abha, Saudi Arabia from March, 2021 to February, 2022.

**Animals:** The scientific ethical committee at King Khalid University oversaw and approved all animal (rat) investigations and this study followed ARRIVE principles. We also confirm that all procedures followed all applicable guidelines and legislation. The trials were conducted on Wistar rats that were 8-10 weeks old and weighed 180-200 g. Rats were kept in a clean place with a 12 hrs light/dark cycle and given free access to food and drink at a constant temperature (22°C) and relative humidity of 50±5%.

**Experimental design and surgical procedures:** A total of 24 rats were randomly assigned to four groups (6 per group) three days after acclimatization: control and three model groups (En5, En10 and En15). The model groups received intratracheal injections of endotoxin (Sigma-Aldrich, MO, USA) while the control group received saline injections. The surgical procedures were carried out exactly as specified<sup>11</sup>. Rats were anaesthetized and each rat was placed in a supine position over a heating blanket to maintain a stable body temperature (37°C). The same midline neck incision was done in rats' groups after confirmation of the third stage of anaesthesia. To see and access the tracheal rings, the platysma and anterior tracheal muscles were dissected away. Using a 1 mL subcutaneous (sub-Q) syringe and a 30 gauge, 5/16-inch needle, 3 mL per gram body weight was instilled into the trachea of each rat. The skin was then sutured (interrupted) in a double layer with the needle tip at a 90° angle around 1-3 mm away from the wound's edge. At the end of the experiment, blood samples were collected under anaesthesia (40 mg kg<sup>-1</sup> sodium thiopentone), rats were culled and lungs were taken.

**Assessment of IL-6, GM-CSF and IL-17A blood levels by ELISA:** The ELISA kits for measuring IL-6 (Invitrogen-Thermo Fisher Scientific, MA, USA), GM-CSF (MyBioSource, San Diego, USA) and IL-17A (MyBioSource, San Diego, USA) were used to measure cytokine levels in plasma samples. All measurements were carried out following guidelines set by the manufacturers.

**Assessment of PT, APTT, PAI-1 and D-Dimer levels:** The APTT and PT were measured as previously disclosed<sup>12</sup>. The PAI-1 was measured using a rat PAI-1 ELISA kit (ab201283) and levels of D-dimer were determined using an ELISA kit (GenWay Biotech, Inc, ca 40-88- 234402, USA).

**Western blotting analysis of GM-CSF and IL-6:** About 20 µg of extracted lung protein per sample were loaded and immunoblotted as previously described<sup>13</sup>. Primary antibodies against rat GM-CSF and IL-6 (R&D Systems, Inc., Minneapolis, MN, USA) were used to probe membranes overnight at 4°C. The ECL detection kit was used to visualize the proteins (Amersham-Pharmacia, UK). After normalization by β-actin on the Chemi Doc MP imager, relative expression was estimated utilizing Image analysis software to read the band intensity of the target proteins against the control sample.

**Histological staining:** Lung samples were collected and fixed in 10% formalin for 24 hrs before being dehydrated with an escalating alcohol grade, followed by cleaning and embedding in paraffin using conventional techniques. To determine the condition of lung architecture and structural alterations, paraffin blocks were sectioned (4  $\mu\text{m}$ ) and stained with hematoxylin and eosin (H&E).

**Immunohistochemistry of iNOS:** Anti-iNOS (Abcam, cat No. ab15323) antibody was used for immunohistochemistry. After antigen retrieval, the main antibody was added and incubated for 12 hrs in a humidity chamber and the tissue was then incubated with the secondary antibody for half an hour. Meyer hematoxylin was used to co-stain the sections.

Morphometry of the percent iNOS positive immunostaining was performed in 10 non-overlapping fields for each group using an image analyzer (Leica Qwin 500 C, Cambridge, UK). The means and Standard Deviations (SD) of quantitative data were calculated and compared using ANOVA and Tukey test. Statistical significance was defined as  $p \leq 0.05$ . The calculations were done using version 19 of SPSS software.

**Statistical analysis:** The data were expressed as the Mean  $\pm$  SD. Statistical analysis was performed using ANOVA and Tukey test. The calculations were done using version 19 of SPSS software. Statistical analysis for two groups was performed using the 2-tailed Student t-test. Results were considered significant if  $p \leq 0.05$ .

## RESULTS

### Activation of inflammatory cytokines by endotoxin

#### A quantitative estimate of achieving a maximal response:

First, the dose of endotoxin was determined that induces maximal cytokine production. We, therefore, administered via intra-tracheal instillation different doses of endotoxin (En), 5, 10 and 15  $\text{mg kg}^{-1}$  into three groups of rats (Fig. 1). A sharp increase ( $p < 0.0001$ ) in the blood levels of inflammatory cytokines; GM-CSF (Fig. 1a), IL-6 (Fig. 1b) and IL-17A (Fig. 1c) was achieved with all three different concentrations of endotoxin when compared with control rats. However, the order of potencies of the endotoxin's effects was:  $\text{En15} > \text{En10} > \text{En5}$ . Having established that En15 is the selected dose, we then assessed lung tissue levels of selected cytokines, GM-CSF and IL-6 using western blots analyses (Fig. 1d-f) and found that it was matching the increase in the observed blood levels.

### Induction of tissue levels of nitrosative stress in rats by

#### endotoxin:

The nitrosative stress biomarker, iNOS is located downstream of the activation of the inflammatory cytokines. Therefore, iNOS protein expression in lung tissues obtained 3 days post endotoxin (En15) injection was assessed (Fig. 2). Using immunohistochemistry, the control group showed a weak positive iNOS immunostaining in the prepared lung sections (Fig. 2a, b). Whereas, the model group (En15) displayed an intense iNOS+ immunostaining in the inflammatory cells infiltrating the interalveolar septa (arrow), in addition to the bronchial epithelium (B) and the endothelium (arrowhead) (Fig. 2c, d). Quantitative analysis of the Mean area (%) of iNOS immunostaining in the lung showed an over 15 fold increase in lung tissue levels of iNOS in the model group (Fig. 2e).

The H&E stained lung sections prepared from the control group showed normal tissue architecture (Fig. 2f) compared with a severe lung tissue damage as demonstrated by the collapse of alveoli (arrowhead), interalveolar septal thickening (I) and desquamated epithelial cells (curved arrow) in the bronchiolar lumen revealed in the model group (Fig. 2g).

### Endotoxin augments coagulation and thrombosis activities

#### in rats:

To determine the extent of coagulation and thrombosis dysregulation induced by endotoxin, blood levels of coagulation and thrombosis biomarkers at the end of the experiment, 72 hrs post endotoxin injection were measured (Fig. 3). Compared with the untreated control rats that showed normal blood values, the model group (En15) caused approximately a three-fold increase in PT (Fig. 3a), a two-fold increase in APTT (Fig. 3b), a five-fold increase in PAI-1 (Fig. 3c) and a ten-fold increase in D-Dimer (Fig. 3d).

### Correlation between iNOS score and biomarkers of inflammation and coagulation and thrombosis:

The correlation between iNOS score and lung tissue and blood levels of GM-CSF, IL-6, IL-17A and PAI-1 was evaluated. This correlation is important in drawing a link between these parameters involved in lung pathology. Nitrosative stress score measured as tissue iNOS displayed a positive correlation with tissue GM-CSF ( $r = 0.989$ ,  $p < 0.0001$ ) (Fig. 4a), tissue IL-6 ( $r = 0.981$ ,  $p < 0.0001$ ) (Fig. 4b), IL-17A ( $r = 0.972$ ,  $p < 0.0001$ ) (Fig. 4c) and PAI-1 ( $r = 0.981$ ,  $p < 0.0001$ ) (Fig. 4d).

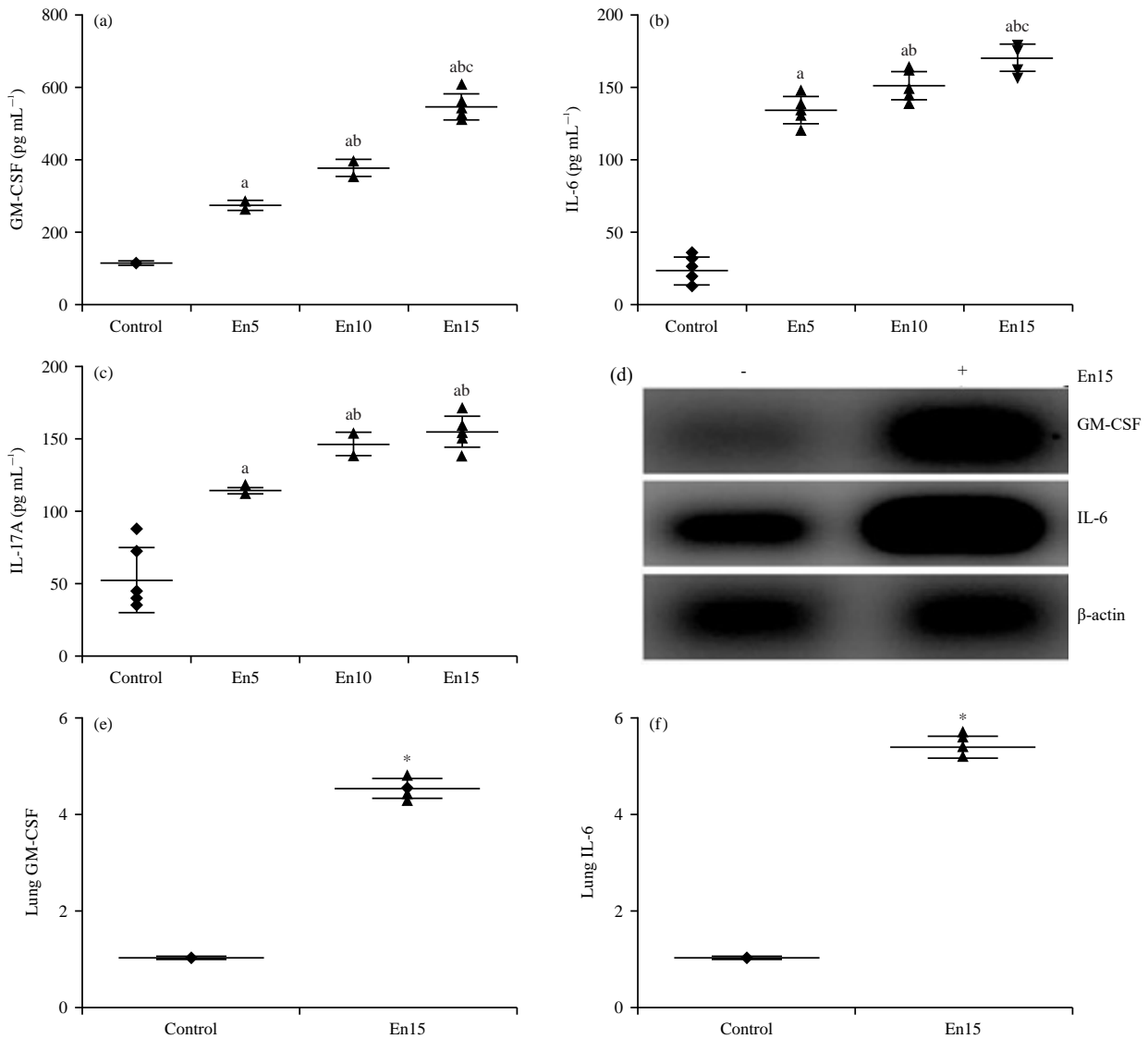


Fig. 1(a-f): Induction of inflammation in rats by endotoxin. Inflammatory cytokine production in response to an increased concentration of endotoxin injections was estimated after three days in the blood of all rat groups for (a) GM-CSF, (b) IL-6 (b) and (c) IL-17A. Expression of lung GM-CSF (d-e), IL-6 (d-f) and b-actin as a loading control (lower bands, d) is shown using immunoblotting analysis.

The presented p-values are all significant. \* $p < 0.05$  vs. control, \* $p < 0.0001$  vs. En5, \* $p < 0.01$  vs. En10, \* $p < 0.01$  vs. En15 and X-axis: Groups

## DISCUSSION

The main objective of this study presented here was to investigate the inflammation/nitrosative stress axis mediated lung injury and dysregulated coagulation and thrombosis induced by a high dose of endotoxin. This study also investigated a correlation between lung iNOS score and inflammation and blood dysregulation. Therefore, different doses of endotoxin were injected via the IT route into rats and all the above parameters were assessed after 3 days. Here, the quantitative estimate of endotoxin dose

(En15) was established that achieved a maximal response for cytokine production (Fig. 1). This dose was able to (i) Increase the protein expression of lung tissue iNOS by >15 fold compared to the control untreated rats (Fig. 2), (ii) Induce substantial lung tissue damage (Fig. 2) and (iii) Cause a sharp increase in coagulation and thrombosis (Fig. 3). Further, the correlation data (Fig. 4) demonstrated the link between inflammation/iNOS axis mediated acute lung injury and dysregulated coagulation and thrombosis. Therefore, the obtained data supported the aim of this study. The data that point to the activation

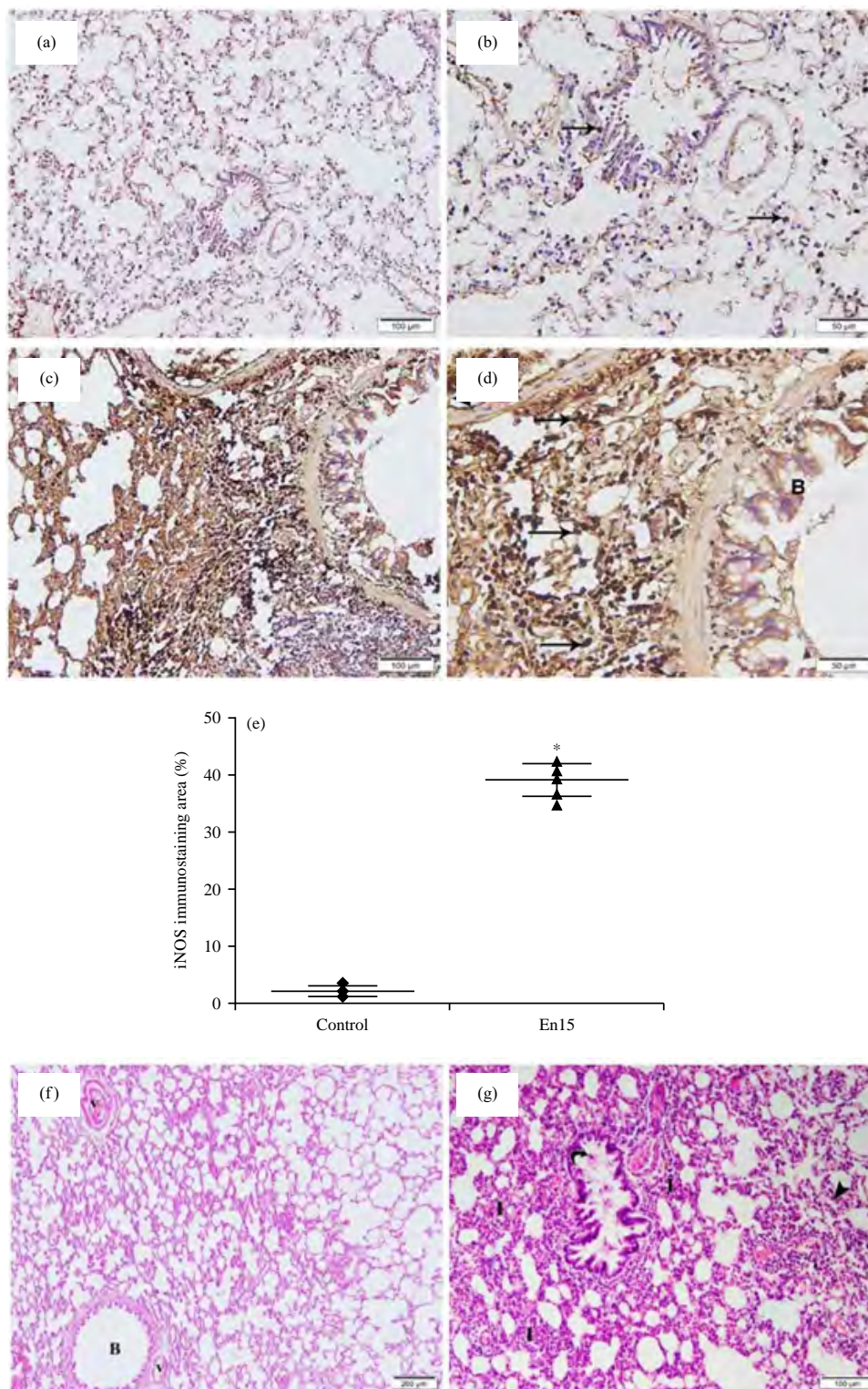


Fig. 2(a-g): Induction of iNOS expression and lung injury in rats by endotoxin, (a-b) iNOS immunohistochemistry of lung sections (x200) prepared from the control rats and (c-d) En15 group are illustrated, (e) A quantitative analysis of iNOS immunostaining area in lung sections from the above rats' groups and (f) H&E stained images (x100) of lung sections from the control rats and (g) the experimental group En15 are shown  
v: Blood vessels, B: bronchioles, \*p<0.05 vs. control and X-axis: Groups

of the inflammation/iNOS axis mediated acute lung injury was in agreement with a previous report that demonstrated the induction of the same axis (inflammation/iNOS) by immobilization stress that induced brain injury<sup>14</sup>.

Endotoxin is widely used in animal models to mimic human diseases like acute respiratory distress syndrome<sup>15</sup>, acute kidney injury caused by the generation of hydrogen

peroxide that induces renal failure<sup>16</sup>, chronic kidney disease and fibrosis due to endotoxemia that caused mTOR activation in macrophages, which induced kidney inflammation<sup>17</sup>, myocardial dysfunction that can lead to increased mortality associated with augmentation of inflammatory cytokines and iNOS expression<sup>18</sup> and acute liver injury due to the reduction of serum IL-22 that has anti-inflammatory and antimicrobial effects<sup>19</sup>.

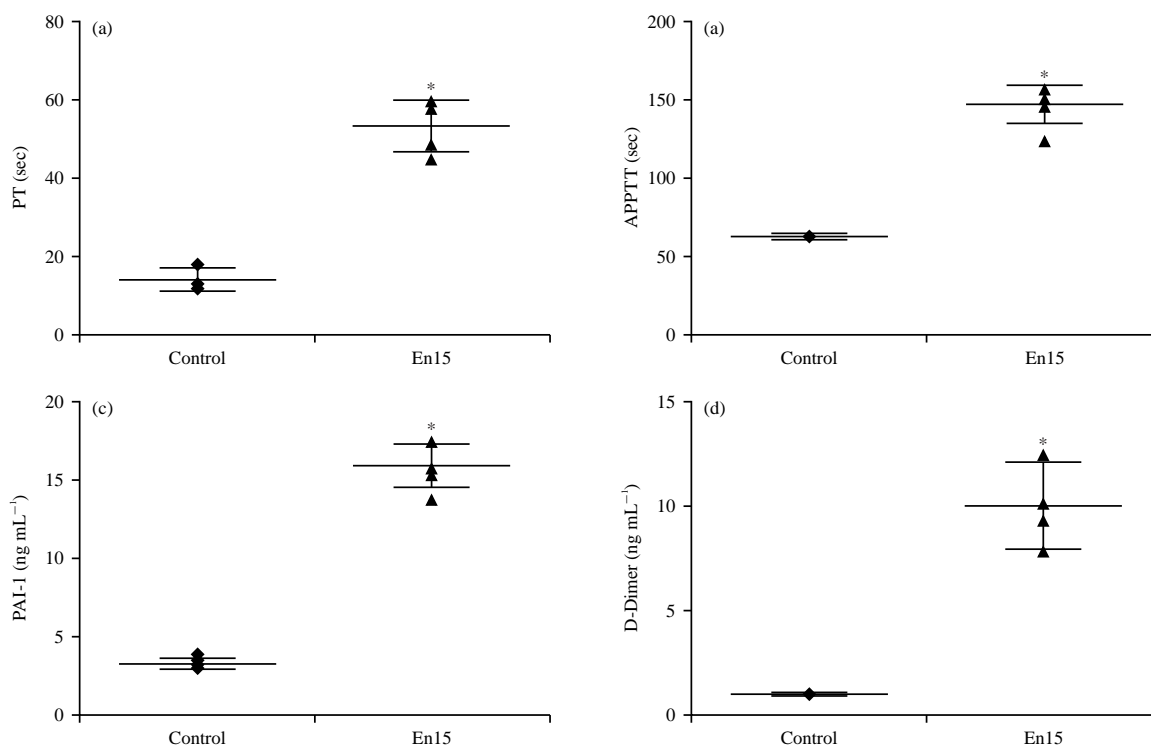


Fig. 3(a-d): Induction of coagulation and thrombosis biomarkers by endotoxin, (a) Coagulation time of blood PT and (b) APTT were assessed 3 days following En15 injection compared with the control rats, (c) Blood levels of PAI-1 and (d) D-dimer are shown in the rat's groups mentioned above

\*p<0.01 vs. control. En15, endotoxin 15 mg kg<sup>-1</sup>, PT: Prothrombin time, APTT: Activated partial thromboplastin time, PAI-1: Plasminogen activator inhibitor-1, D-dimer: Degradation product of cross-linked fibrin and X-axis: Groups

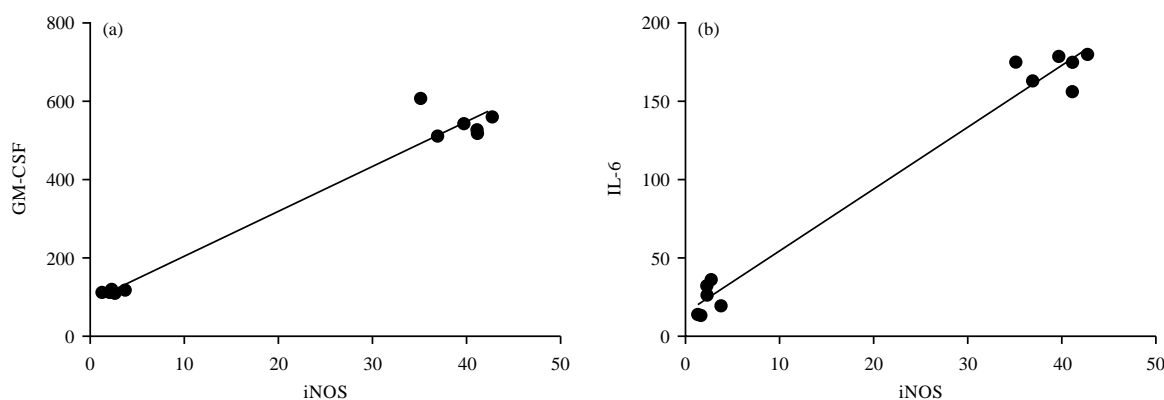


Fig. 4(a-d): Continue

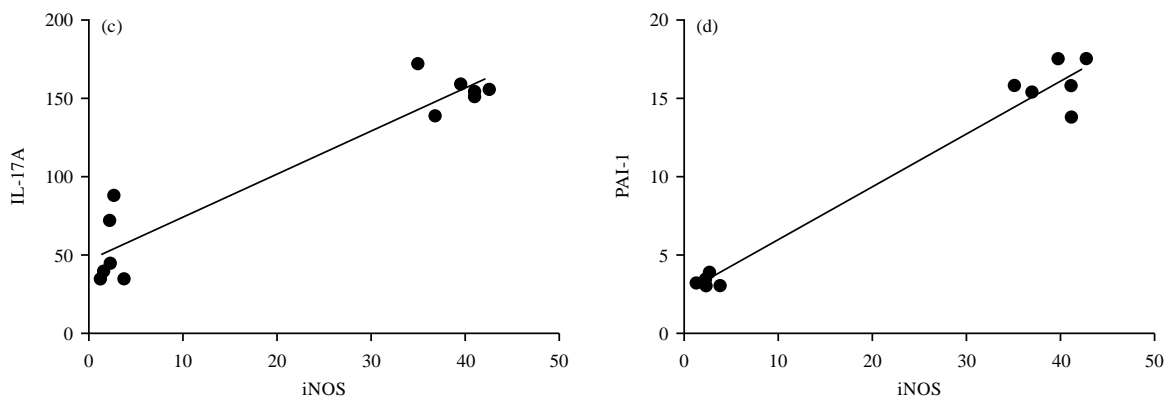


Fig. 4(a-d): Correlation between the scoring of iNOS and biomarkers of inflammation and coagulation and thrombosis. After experiment completion, the degree of nitrosative stress measured as iNOS lung expression was assessed in rats and the relationship between (a) iNOS and GM-CSF, (b) IL-6, (c) IL-17A and (d) PAI-1 is shown

Furthermore, endotoxin augmented carbon tetrachloride (CCl<sub>4</sub>)- and alcohol-induced liver injury and administration of anti-endotoxin antibody E5 blocked liver injury caused by CCl<sub>4</sub> and alcohol<sup>20</sup>. These reports were in accord with current findings that demonstrated the activation of inflammation/iNOS axis mediated acute lung injury by the high dose of endotoxin in rats.

### CONCLUSION

Collectively, using an acute lung injury rat model induced by a high endotoxin dose, these findings demonstrated a link between the inflammation/iNOS mediated acute lung injury and dysregulated coagulation and thrombosis after 3 days, which may offer to test therapeutic compounds for the treatment of severe acute lung damage.

### SIGNIFICANCE STATEMENT

This study represents a significant contribution to the study of severe acute lung injury induced in rats by IT injection of a high dose of endotoxin over three days since it investigates the inflammation/nitrosative stress signalling molecules in lung tissue exposed to endotoxin associated with lung injury and dysregulated coagulation and thrombosis, which can be a useful animal model exposed to endotoxin for a relatively 'long' period.

### ACKNOWLEDGMENTS

We are grateful to Prof. Bahjat Al-Ani from the Physiology Department, College of Medicine, King Khalid University, Abha, Saudi Arabia and Dr. Samaa S. Kamar from the

Department of Medical Histology, Kasr Al-Aini Faculty of Medicine, Cairo University, Cairo, Egypt for their help and support. Also, we thank Dr. Mariam Al-Ani from Face Studio Clinic, 90 Hagley Road, Edgbaston, Birmingham, B16 8LU, the UK for proofreading the manuscript. This work was funded by Princess Nourah Bint Abdulrahman University Researchers Supporting Project number (PNURSP2022R110), Princess Nourah Bint Abdulrahman University, Riyadh, Saudi Arabia. This research was also funded by the Research Deanship of King Khalid University, Abha, Saudi Arabia; Grant number No. GRP-215-43.

### REFERENCES

1. Matthay, M.A. and R.L. Zemans, 2011. The acute respiratory distress syndrome: Pathogenesis and treatment. *Annu. Rev. Pathol. Mech. Dis.*, 6: 147-163.
2. Chiumello, D., S. Froio, B. Bouhemad, L. Camporota and S. Coppola, 2013. Clinical review: Lung imaging in acute respiratory distress syndrome patients - An update. *Crit. Care*, Vol. 17. 10.1186/cc13114.
3. Han, S. and R.K. Mallampalli, 2015. The acute respiratory distress syndrome: From mechanism to translation. *J. Immunol.*, 194: 855-860.
4. Frantzeskaki, F., A. Armaganidis and S.E. Orfanos, 2017. Immunothrombosis in acute respiratory distress syndrome: Cross talks between inflammation and coagulation. *Respiration*, 93: 212-225.
5. Wang, H.M., M. Bodenstern and K. Markstaller, 2008. Overview of the pathology of three widely used animal models of acute lung injury. *Eur. Surg. Res.*, 40: 305-316.
6. Rittirsch, D., M.A. Flierl, D.E. Day, B.A. Nadeau and S.R. McGuire *et al.*, 2008. Acute lung injury induced by lipopolysaccharide is independent of complement activation. *J. Immunol.*, 180: 7664-7672.



7. Gielis, J.F., P.A.J. Beckers, J.J. Briedé, P. Cos and P.E. van Schil, 2017. Oxidative and nitrosative stress during pulmonary ischemia-reperfusion injury: From the lab to the OR. *Ann. Transl. Med.*, Vol. 5. 10.21037/atm.2017.03.32.
8. Malaviya, R., A. Venosa, L. Hall, A.J. Gow, P.J. Sinko, J.D. Laskin and D.L. Laskin, 2012. Attenuation of acute nitrogen mustard-induced lung injury, inflammation and fibrogenesis by a nitric oxide synthase inhibitor. *Toxicol. Appl. Pharmacol.*, 265: 279-291.
9. Tufvesson, E., C. Andersson, J. Weidner, J.S. Erjefält and L. Bjermer, 2017. Inducible nitric oxide synthase expression is increased in the alveolar compartment of asthmatic patients. *Allergy*, 72: 627-635.
10. Pitt, B.R. and C.M.S. Croix, 2002. Complex regulation of iNOS in lung. *Am. J. Respir. Cell Mol. Biol.*, 26: 6-9.
11. Helms, M.N., E. Torres-Gonzalez, P. Goodson and M. Rojas, 2010. Direct tracheal instillation of solutes into mouse lung. *J. Vis. Exp.*, Vol. 29. 10.3791/1941
12. Rizzo, F., K. Papisoulitis, E. Crawford, S. Dodkin and S. Cue, 2008. Measurement of prothrombin time (PT) and activated partial thromboplastin time (APTT) on canine citrated plasma samples following different storage conditions. *Res. Vet. Sci.*, 85: 166-170.
13. Al Hashem, F., S. Al Humayed, S.N. Amin, S.S. Kamar and S.S. Mansy *et al.*, 2019. Metformin inhibits mTOR-HIF 1 $\alpha$  axis and profibrogenic and inflammatory biomarkers in thioacetamide-induced hepatic tissue alterations. *J. Cell. Physiol.*, 234: 9328-9337.
14. Madrigal, J.L.M., O. Hurtado, M.A. Moro, I. Lizasoain and P. Lorenzo *et al.*, 2002. The increase in TNF- $\alpha$  levels is implicated in NF- $\kappa$ B activation and inducible nitric oxide synthase expression in brain cortex after immobilization stress. *Neuropsychopharmacology*, 26: 155-163.
15. Zhang, H.X., S.J. Liu, X.L. Tang, G.L. Duan and X. Ni *et al.*, 2016. H<sub>2</sub>S attenuates LPS-induced acute lung injury by reducing oxidative/nitritative stress and inflammation. *Cell Physiol. Biochem.*, 40: 1603-1612.
16. Yoo, J.Y., D.R. Cha, B. Kim, E.J. An, S.R. Lee *et al.*, 2020. LPS-induced acute kidney injury is mediated by Nox4-SH3YL1. *Cell Rep.*, Vol. 33. 10.1016/j.celrep.2020.108245.
17. Chen, H., J. Zhu, Y. Liu, Z. Dong and H. Liu *et al.*, 2015. Lipopolysaccharide induces chronic kidney injury and fibrosis through activation of mTOR signaling in macrophages. *Am. J. Nephrol.*, 42: 305-317.
18. Zhang, N., H. Feng, H.H. Liao, S. Chen, Z. Yang, W. Deng and Q.Z. Tang, 2018. Myricetin attenuated LPS induced cardiac injury *in vivo* and *in vitro*. *Phytother. Res.*, 32: 459-470.
19. Shao, L., X. Xiong, Y. Zhang, H. Miao and Y. Ren *et al.*, 2020. IL-22 ameliorates LPS-induced acute liver injury by autophagy activation through ATF4-ATG7 signaling. *Cell Death Dis.*, Vol. 10.1038/s41419-020-03176-4.
20. Su, G.L., S.M. Goyert, M.H. Fan, A. Aminlari, K.Q. Gong *et al.*, 2002. Activation of human and mouse Kupffer cells by lipopolysaccharide is mediated by CD14. *Am. J. Physiol. Gastrointestinal Liver Physiol.*, 283: G640-G645.